J. Fluid Mech. (1988), *vol.* 196, *pp.* 467–494
Printed in Great Britain

A study of forces, circulation and vortex patterns around a circular cylinder in oscillating flow

By E. D. OBASAJU†, P. W. BEARMAN‡ AND J. M. R. GRAHAM‡

† British Maritime Technology Ltd, Teddington, Middlesex, UK

‡ Department of Aeronautics, Imperial College, London SW7, UK

(Received 15 September 1986 and in revised form 25 November 1987)

Measurements of sectional and total forces and the spanwise correlation of vortex shedding are presented for a circular cylinder in planar oscillatory flow at Keulegan–Carpenter numbers, KC, in the range from about 4 to 55. The viscous parameter β is in the range from around 100 to 1665. Circulation measurements around a circuit close to and enclosing the cylinder, are also presented. A mode-averaging technique was used for both sectional forces and circulation measurements and this gave, for typical modes of vortex shedding, time histories over an average cycle. The transverse force and the circulation tend to fluctuate in sympathy with each other, except around the instant of flow reversal when the force changes sign but the circulation remains high. Values of the strength of shed vortices, estimated from the measured circulation, are found to be comparable with steady-flow results. For $KC \lesssim 30$, modes of vortex shedding occur over distinct ranges of KC with spanwise correlation high at the centre of a KC-range for a particular mode of shedding but low at the boundaries. Above $KC \approx 30$ the correlation is no longer very sensitive to KC and the correlation length is estimated to be equal to 4.65 cylinder diameters. In the transverse vortex-street regime ($8 \lesssim KC \lesssim 15$) the cylinder was found to experience a steady transverse force, the coefficient of which is estimated to be about 0.5 at $KC = 14$.

1. Introduction

The flow around a circular cylinder with relative sinusoidal motion along a diameter is a function of the Keulegan–Carpenter number KC and the Reynolds number R_e. Here $KC = 2\pi A/D$, where A is the amplitude of the motion and D is the cylinder diameter. The Reynolds number is based on D and the maximum velocity of the cylinder, U_0. Hence $R_e = KC\,(D^2/\nu T)$, where ν is the kinematic viscosity and T is the period of the cylinder motion. Following Sarpkaya (1976) the viscous parameter, $D^2/\nu T$, will be denoted by β. When KC is sufficiently small, the boundary layer on an oscillating cylinder is everywhere attached, laminar, stable and two-dimensional. The only force on the cylinder is directed along the line of motion and has been given (e.g. Stokes 1851; Wang 1968) as a function of β. As KC increases, it appears (Honji 1981; Sarpkaya 1986) that the laminar boundary-layer flow becomes unstable, forming three-dimensional vortices along the cylinder span. Sarpkaya (1986) has shown that if β is less than about 2600, this instability is followed by boundary-layer separation and then transition of the separated shear layer from laminar to turbulent flow; whereas for larger β, transition occurs within the boundary layer before flow separation. When KC is large, the separated shear layers form vortices with a size of the order of the cylinder diameter. When these vortices

form asymmetrically they lead to an additional force transverse to the flow direction. Depending on KC some or all of the shed vorticity is swept back past the cylinder during flow reversal. The result is an extremely complex flow field which is not directly amenable to theoretical solution.

This paper describes the development of the flow from $KC \approx 4$, where transverse forces are first observed, to KC of about 60, and is a companion to the paper by Bearman *et al.* (1985) which concentrates on low-KC flow (i.e. $KC \lesssim 10$). The understanding of this class of flow has received considerable attention because of the need to predict wave forces on offshore structures. A comprehensive review of earlier studies has been given by Sarpkaya & Isaacson (1981). The majority of the previous research has been directed towards the in-line force, and the usual practice has been to represent this force by Morison's equation (Morison *et al.* 1950):

$$F = \tfrac{1}{2}\rho D U |U| C_{\mathrm{D}} + \tfrac{1}{4}\pi\rho D^2 \frac{\mathrm{d}U}{\mathrm{d}t} C_{\mathrm{M}}, \tag{1}$$

where F is the in-line force per unit length of the cylinder, and U is the velocity of the imposed relative motion. C_{D} and C_{M} are drag and inertia coefficients respectively, and are functions of KC and β (for example see Keulegan & Carpenter 1958 and Sarpkaya 1976).

The transverse force is more difficult to analyse since it is more sensitive to the ways in which vortices are formed and move. Several authors have proposed ranges of KC for particular types of vortex-shedding behaviour (Singh 1979; Sarpkaya & Isaacson 1981; Bearman *et al.* 1981; Iwagaki, Asano & Nagai 1983; Williamson 1985). An indication of the complexity of the flow is given by the fact that Iwagaki *et al.* (1983) suggested that the range of KC from 2.9 to about 30 be separated into eight regimes. Even when KC and β are fixed, more than one mode of shedding is possible, and the flow may switch between the possible modes – see Bearman *et al.* (1981). Most of the experimental information available on traverse forces relates to the dominant frequency and the maximum value of the force. It has been suggested by several authors that if detailed information on vortex strengths and motion are available then the Blasius equation can be used to calculate the development of both in-line and transverse forces. Using this equation Maull & Milliner (1978) have described qualitatively how the development of transverse and in-line forces can be related to the generation and movement of vortices. This idea has also been used by Ikeda & Yamamoto (1981), and by Williamson (1985). The former estimated the motion and strength of vortices from photographs and used the results to make rough predictions of the development of the transverse force. The initial motivation for the work described here was the desire to acquire information that could be used to test this approach and that might provide a better understanding of the role of vortices in fluid loading.

As a first step towards achieving this objective, it was necessary to develop a scheme for obtaining average cycles of the time history of the transverse force for different modes of vortex shedding. The mode-averaging scheme adopted for this purpose will be described fully in §2. Preliminary results have been presented in Bearman *et al.* (1981), together with a quasi-steady model for predicting the development of a transverse force. This model assumes that during a flow cycle the Strouhal number $S = fD/U$, formed from instantaneous values of the vortex-shedding frequency f and the flow velocity, is constant. Over the range of Reynolds number studied here the data is well fitted with $S = 0.2$, which is the value

appropriate to steady flow at the same Reynolds number. A similar model was proposed by Verley (1982) but he did not make quantitative comparisons with experimental data. A full description of the quasi-steady model is given by Bearman, Graham & Obasaju (1984) where comparisons of time histories between theory and measurement are made down to KC-values of about 6. It was found that even at low KC where the prediction of the model is, as expected, less good, the frequency of the transverse force is still quite well represented with a Strouhal number of 0.2. These preliminary studies indicated that even though many different vortex patterns are exhibited in oscillatory flow, the basic mechanism that governs the rate at which vortices develop may be the same as in steady flow.

In this paper, we aim to extend the research reviewed above and to consider a number of issues raised by Bearman *et al.* (1981). They reported that, contrary to what is sometimes supposed, the spanwise correlation of vortex shedding in planar oscillatory flow may be poor, even at low KC. They showed that at KC-values of about 10 a sideways vortex street develops and they speculated that in addition to the unsteady transverse force, the cylinder may also experience a time-mean transverse force. We report on the use of the mode-averaging technique to make measurements of the circulation around a circuit enclosing the cylinder. The time history of this circulation will be compared with that of the transverse force. Hopefully such information will provide a better physical understanding and help in the development of more realistic numerical models.

2. Experimental arrangement

2.1. *Description of experiments*

Planar oscillatory flow was realized by utilizing the resonance of a U-tube water tunnel with a fixed cylinder immersed in the flow and also by oscillating a model in a water channel. The U-tube has been described fully by Singh (1979). The working section, which is in the horizontal limb of the tube, is 0.61 m square and 1.5 m long. The period, T, of oscillation of the water in the U-tube is 3.34 s. The amplitude can be varied up to 0.6 m peak-to-peak. Constant-amplitude oscillations are maintained by an air blower, attached to one of the vertical limbs, which is controlled using the signal from a capacitance gauge recording the instantaneous water level.

Two series of measurements were made in the U-tube. For the first set, the model was supported at each end on strain-gauged load cells, flush with the walls of the tube. These measured the total force experienced by the model. Experiments were carried out on seven circular cylinders with diameters ranging from 1.91 to 7.48 cm, giving values of β between 109 and 1665. The water-level and force signals were recorded simultaneously on an analogue tape recorder and then discretized and processed on a digital computer.

The purpose of the second series of U-tube measurements was to determine the force acting on a small length of the cylinder and to estimate the circulation around it. A circular cylinder with a diameter of 3.73 cm, giving $\beta = 416$, was used for these measurements. The cylinder had two pressure tappings at mid-span placed diametrically opposite each other. Each tapping was connected to a Setra 237 pressure transducer with a range of 5 psi. Velocity measurements around the cylinder at its centre span were made using a Thermo Systems laser anemometer working in forward scatter with a frequency tracker. The velocity and water-level signals, and the difference between the pressures observed at the two tappings were recorded simultaneously on the analogue tape recorder. Recordings were made for at least 150

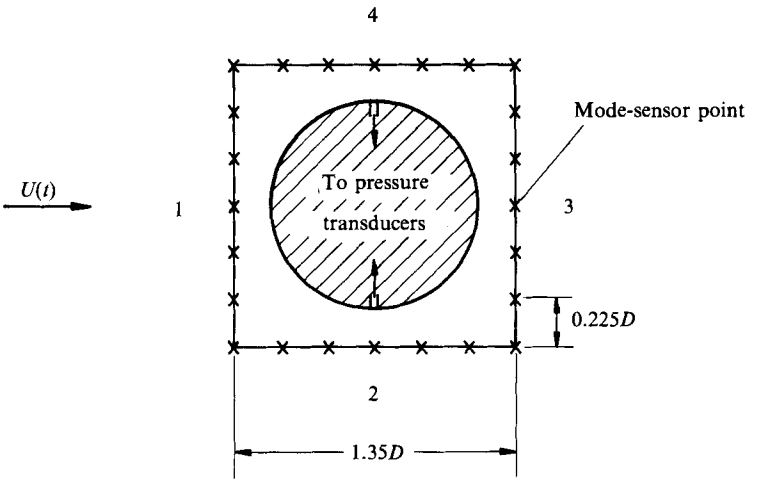

FIGURE 1. Conditional-averaging scheme.

cycles of water oscillation. In order to estimate the sectional force from the pressure measurements, recordings of velocity were made at a fixed point (the mode-sensor point in figure 1) while recordings of the pressure difference were made with the pair of tappings set at each of 12 equally spaced angular positions around the cylinder. The velocity measurement points used to estimate the circulation are also shown in figure 1 (*a*). The pressure difference across the cylinder at $\pm 90°$ to the main flow was recorded while velocity measurements were made at points (indicated by crosses in figure 1) on a square circuit surrounding the cylinder. The horizontal component of velocity was measured on the horizontal parts (sides 2 and 4) of the circuit and the vertical components on the remaining parts. The circulation round the circuit was estimated from an integration of the measured velocities.

The other facility used to generate planar oscillatory flow was an open water channel. The working section of this channel is 0.61 m wide, 0.68 m deep, and 3 m long. Above the working section there is a carriage which can be driven in sinusoidal motion. The motion of the carriage is monitored by a displacement transducer. The frequency of oscillation can be varied up to a maximum of about 1 Hz and the amplitude in steps of 2.54 cm between 6.35 cm and 31.75 cm. Models are mounted vertically in the channel. In this investigation the top end of each model was clamped to the carriage and the bottom end was about 1 cm above the floor of the channel. The diameter of the models used was 4 cm. Two thin circular end plates, 32 cm in diameter and with chamfered edges, were attached to each model. The distance between the plates was equal to just over $9.5D$.

Two circular-cylinder models were tested in the channel. Each model had pairs of pressure tappings with the tappings forming a pair placed diametrically opposite each other. One model was used to investigate the forces acting at a cross-section of the cylinder and the tappings were located at mid-span between the end plates. The other model was used to investigate the correlation of the fluctuating transverse force and the tappings were distributed on two diametrically opposite lines running along the length of the model. The pairs of tappings were led to two pairs of pressure transducers which were mounted on the carriage. The outputs of the transducers forming a pair were subtracted from each other and the resulting pressure-difference

signals from two pairs were recorded simultaneously with the displacement signal. In the case of the sectional-force measurements, the pressure difference across the oscillating cylinder at $\pm 90°$ to the line of motion was always monitored while pressure measurements were made at other angular positions around the cylinder. As in the U-tube, sectional forces were estimated from measurements made at twelve equally spaced angular positions around the cylinder. In the case of the correlation measurements, the two rows of tappings on the model were set at $\pm 90°$ to the line of motion.

2.2. *The mode-averaging technique*

The aim is to obtain average cycles of the transverse force but problems arise because at a given KC the flow can switch between different vortex-shedding modes. Furthermore each mode is usually associated with a mirror-image mode which generates lift of roughly the same magnitude but of opposite sign. Hence when a large number of cycles of the transverse force are ensemble-averaged the result is almost zero – see Bearman *et al.* (1981). To obtain more meaningful averages some method for recognizing the flow state is required.

In this paper the flow mode has been inferred from the characteristics of two different signals referred to as the mode-sensor signals. The positions of the mode sensors are shown in figure 1. For the pressure measurements made in the U-tube, the mode sensor is the transverse component of velocity measured on the centreline of the flow near the face of the cylinder. For the remaining measurements (i.e. circulation measurements in the U-tube and pressure measurements in the channel) the mode sensor is taken as the pressure difference across the cylinder at $\pm 90°$ to the line of motion. In each averaging scheme, the mode-sensor signal is Fourier analysed at frequencies that are multiples of the oscillation frequency and cycles are sorted according to both the dominant frequency and phase. Phase is important because two cycles may generate similar frequency information but their vortex-shedding patterns may be in antiphase.

The type of analysis from which flow modes are determined is illustrated in figure 2. For the case shown, $KC = 17.5$ and the mode sensor is the velocity signal. The component, F_m, of the mode-sensor signal at a dominant frequency, m, is defined as

$$F_m = A_m \sin 2\pi mt + B_m \cos 2\pi mt, \tag{2}$$

and a phase angle ϕ is given by

$$\phi = \tan^{-1}(A_m/B_m). \tag{3}$$

For a particular frequency, a number density function, $P(\phi)$ is computed, defined as

$$\frac{\text{Number of cycles for which } \phi \text{ lies in the range } \phi - \frac{1}{2}\Delta\phi_0 \leqslant \phi \leqslant \phi + \frac{1}{2}\Delta\phi_0}{(\text{Total number of cycles}) \times \Delta\phi_0},$$

where $\Delta\phi_0$ is the bandwidth used for the analysis. $P(\phi)$ as a function of ϕ is plotted in figure 2 for dominant frequencies of N, $2N$, $3N$ and $4N$, where N is the water oscillation frequency. For the case illustrated the percentage of the number of cycles for which these frequencies were dominant are 25 %, 13 %, 58 % and 2 % respectively. The total number of cycles analysed to generate figure 2 was 2440 and $\Delta\phi_0 = 10°$. It is seen that at a given dominant frequency, $P(\phi)$ has two peaks separated by approximately 180°. At high KC ($KC \gtrsim 30$) peaks in $P(\phi)$ tended to be less marked but are still discernible. In the basic mode-averaging scheme, each peak was treated as a separate flow mode, and cases for which the phase angle lay within 30° of a peak were ensemble-averaged as one mode.

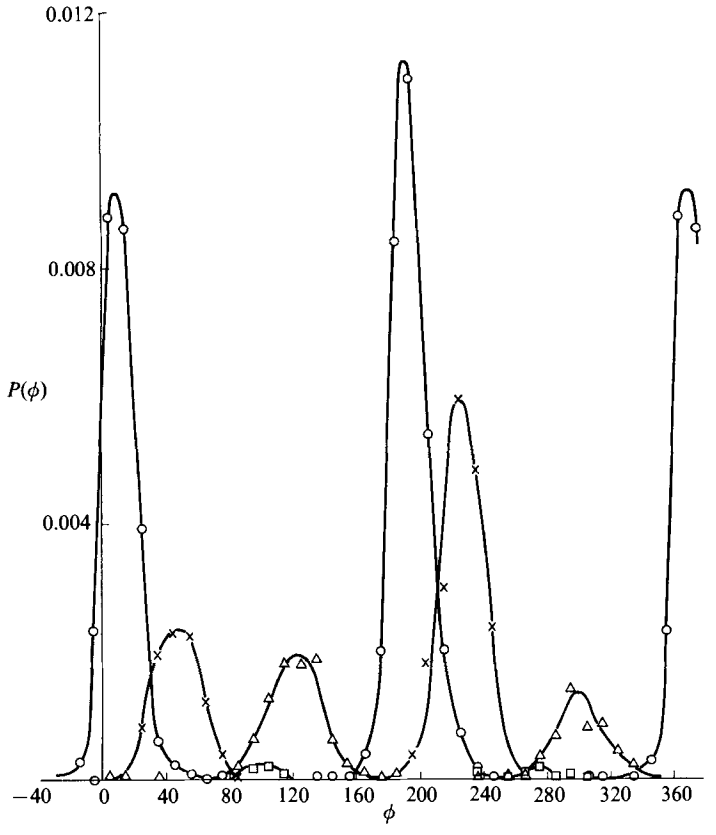

FIGURE 2. Number density functions, calculated from the transverse velocity close to a stagnation point, at $KC = 17.5$. Dominant frequency: ×, N; △, $2N$; ○, $3N$; □, $4N$.

Although useful results were obtained by using the averaging scheme outlined above, it sometimes failed to detect all the modes. For example, flow visualization in the U-tube at $KC \approx 10$ shows that one vortex pair is shed in every cycle of the tank and that the pair can convect along four paths, namely $\theta \approx 45°$, $135°$, $-45°$, and $-135°$, where θ is the angle between the vortex path and the positive direction of the main flow. Hence there are four basic vortex-shedding modes. The pressure difference across the cylinder at $\pm 90°$ to the line of motion showed that at $KC = 10$ the dominant frequency was always $2N$. At this frequency, $P(\phi)$ has two sharp peaks separated by a phase angle of about 180°. Hence the basic averaging scheme indicated that there were only two modes. Analysis at other harmonics of the oscillation frequency showed that phase angles were also concentrated around two values separated by 180°. It was found that the four modes could be resolved by combining the phase information recorded at two frequencies, one of which is an even multiple of the tank oscillation frequency, the other odd. This concept has been incorporated into the mode-averaging scheme.

3. Results

3.1. *Flow visualization*

The range of KC from about 3 to 55 can be divided into the following regimes: $KC \lesssim 4$, $4 \lesssim KC \lesssim 8$, $8 \lesssim KC \lesssim 15$, $15 \lesssim KC \lesssim 22$, $22 \lesssim KC \lesssim 30$, and $KC \gtrsim 30$.

Following Singh (1979) and Bearman *et al.* (1981), the first four regimes will be called the symmetric, the asymmetric, the transverse, and the diagonal regimes respectively. The regime $KC \geqslant 30$ will be called the quasi-steady regime. The main difference between the above classification scheme and the one given by Bearman *et al.* (1981) is that the diagonal regime is now coupled to the quasi-steady regime by a new regime, namely $22 \lesssim KC \lesssim 30$. In the new regime, three full vortices are shed per half-cycle and Sawameto and Kikuchi (see Iwagaki *et al.* 1983) have called this regime the third vortex regime. The regime boundaries agree approximately with those suggested by Williamson (1985). He reported that an increment of about 8 in KC generates one more vortex per half-cycle and hence a new vortex pattern. The quasi-steady regime can, therefore, be subdivided into additional regimes.

Singh (1979) and Williamson (1985) performed extensive visualization studies of the flow around bluff bodies in oscillatory flow and have described the main features in each regime. We have carried out further flow visualizations at $KC \approx 7$, 10 and 18 where some of our more detailed measurements were made. Like Singh (1979), the flow was visualized by using small polystyrene particles illuminated by narrow slits of light. The visualization was performed in the U-tube at $\beta = 416$. Figure 3 (*a*) shows sketches of the vortex patterns observed in the asymmetric regime at $KC \approx 7$. It is seen that vortex activity tends to be concentrated on one side of the cylinder (the upper side in the sketches). A shed vortex, formed in the previous half-cycle and carried back during flow reversal, is present in each half of the motion. The shed vortex remains close to the cylinder and seems to be dissipated as it is carried back towards the cylinder during flow reversal – see the middle sketch in figure 3 (*a*). Vortex patterns observed in the transverse regime at $KC \approx 10$ are sketched in figure 3 (*b*). Vortex activity is one-sided and two vortices with opposite signs are again shed in one complete cycle. The shed vortices now form a pair and are able to convect to large distances from the model. In the diagonal regime at $KC \approx 18$ (figure 3*c*) a pair of vortices is shed in each half-cycle and the vortex pair in the one half-cycle is shed diametrically opposite to the pair in the previous half-cycle. In both the transverse and the diagonal regimes, vortex pairs convect at about 45° to the main flow, when viewed with the cylinder fixed.

It follows, because of the possibility of mirror-image modes, that there are two primary modes in the asymmetric and diagonal regimes. As discussed in the previous section, there are four primary modes in the transverse regime. It was observed that a vortex pattern can be stable over a large number of cycles and then change from one mode to another. Measurements have revealed that the change does not occur abruptly and that as a consequence, a large variety of secondary (i.e. combination) modes can be generated. In these circumstances the number of modes identified will depend to some extent on how strictly the mode selection criteria are applied. At some KC-values on the boundaries between regimes, up to 10 modes could be identified. In this paper, we shall be concentrating only on the predominant modes. The fraction, P, of the total number of cycles belonging to the predominant mode, including its mirror image, is given in Bearman *et al.* (1984). P was found to range from about unity at $KC \approx 10$ to 0.35 at $KC \approx 50$.

An interesting observation was made in the U-tube at $KC \approx 10$. Vortices can form either in phase along the cylinder or in two apparently independent cells. In the case of the two-cell structure, each cell occupies about half the span of the cylinder and in this state a vortex pair moved towards the roof of the U-tube in one cell and approached the floor in the other. The pair approaching the floor cleared away particles on the floor over about half the width of the tank. Two types of shedding

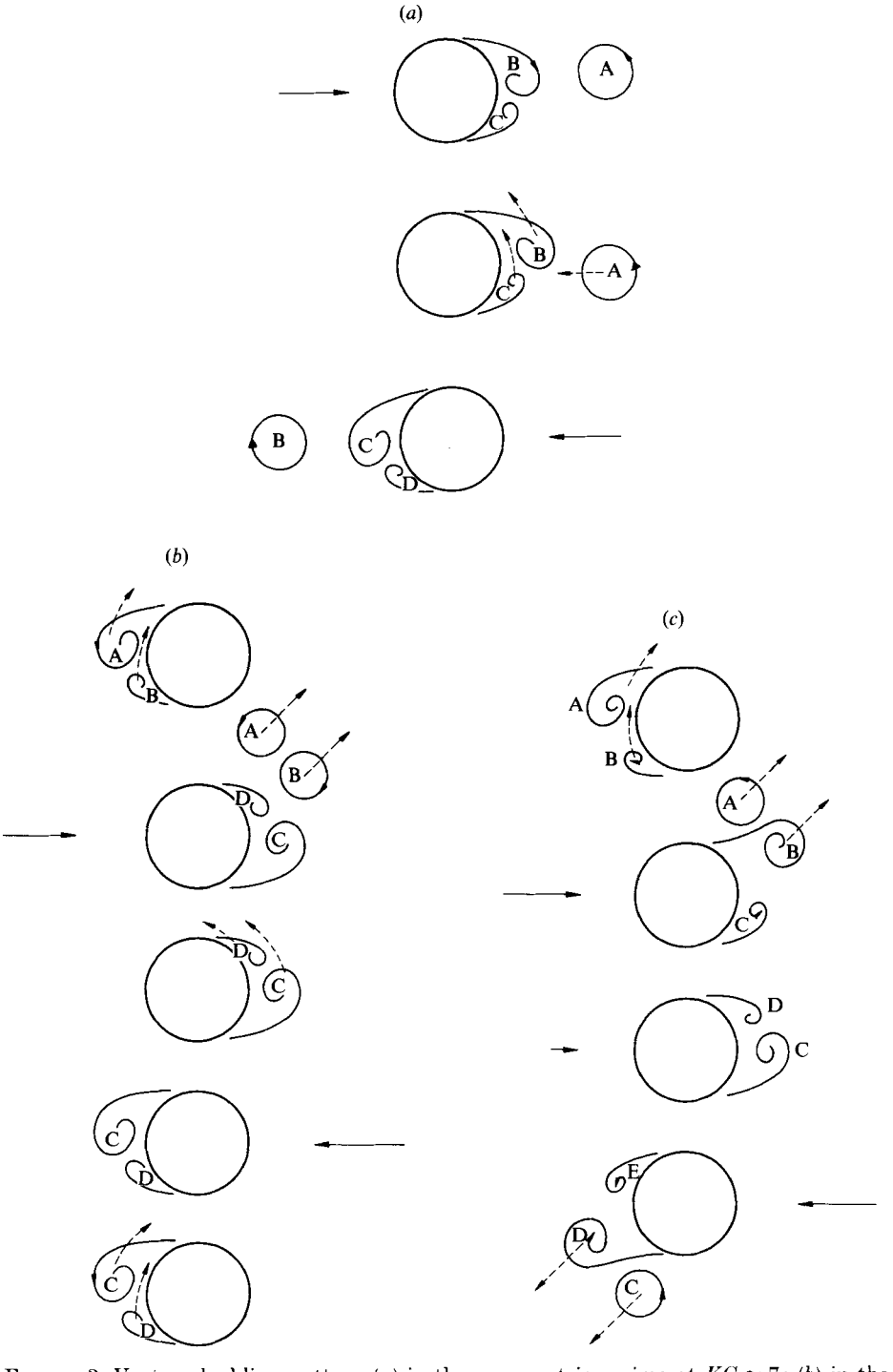

FIGURE 3. Vortex-shedding pattern (*a*) in the asymmetric regime at $KC \approx 7$; (*b*) in the transverse regime at $KC \approx 10$; (*c*) in the diagonal regime at $KC \approx 18$.

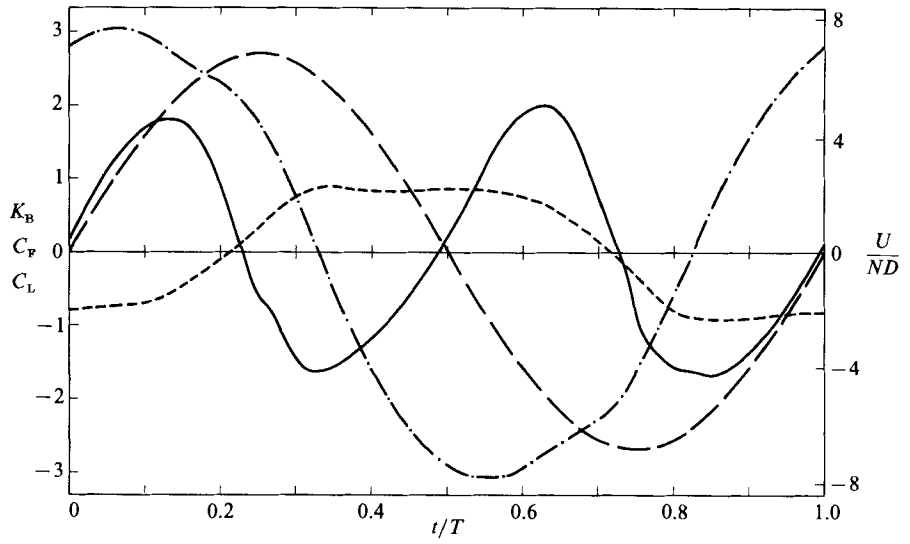

FIGURE 4. Mode-averaged cycles of forces and circulation at $KC = 6.75$: —·—, in-line force coefficient; ——, transverse force coefficient; – – –, non-dimensional circulation; — —, free-stream relative velocity.

can also be observed by studying the signals from the transverse-force transducers. When the single-cell structure is formed, the transverse-force signal is regular in amplitude and frequency whereas in the case of the two-cell structure the signal is, probably as a result of movement of the boundary separating the two cells, irregular and intermittent. After the water in the U-tube is set into motion either of the two flow states can be set up. Once set up, the single-cell structure seems to persist whereas the two-cell structure can sometimes collapse into a single cell.

3.2. *Sectional forces and circulation*

Figures 4–12 show time histories of mode-averaged data. In each figure, mode-averaged values of the transverse and in-line force coefficients, C_L and C_F respectively, calculated from pressure distributions, are plotted against t/T, where t is time and T is the period of oscillation. Coefficients have been formed by dividing the sectional forces by $\frac{1}{2}\rho U_0^2 D$, where U_0 is the amplitude of U, the free-stream velocity relative to the cylinder. The curve of U/ND versus t/T, where N is the frequency of the main flow, is shown in each figure. It should be noted that a half-cycle is the period between two consecutive flow reversals, and thus a half-cycle begins and ends when $U/ND = 0$. Also shown in figures 4, 6 and 8 are time histories of the circulation, Γ_B, measured round the square circuit described in §2. Clearly the value of the circulation will depend upon the circuit chosen and will be zero for a circuit coinciding with the cylinder surface and zero for a very large circuit. The circuit used in this investigation encloses the vorticity associated with the near flow around the cylinder and is unlikely to contain much of the vorticity associated with vortices that have been shed. Note that anticlockwise circulation is positive and that Γ_B has been non-dimensionalized by dividing by $U_0 D$, i.e. $K_B = \Gamma_B/U_0 D$.

The mode shown in each of the above figures is normally the predominant one. Exceptions are figures 6(*a*) and 9(*a*, *b*). In figure 6(*a*) we demonstrate the usefulness of mode averaging by showing results obtained at $KC = 17.5$. C_L, C_F, and K_B are

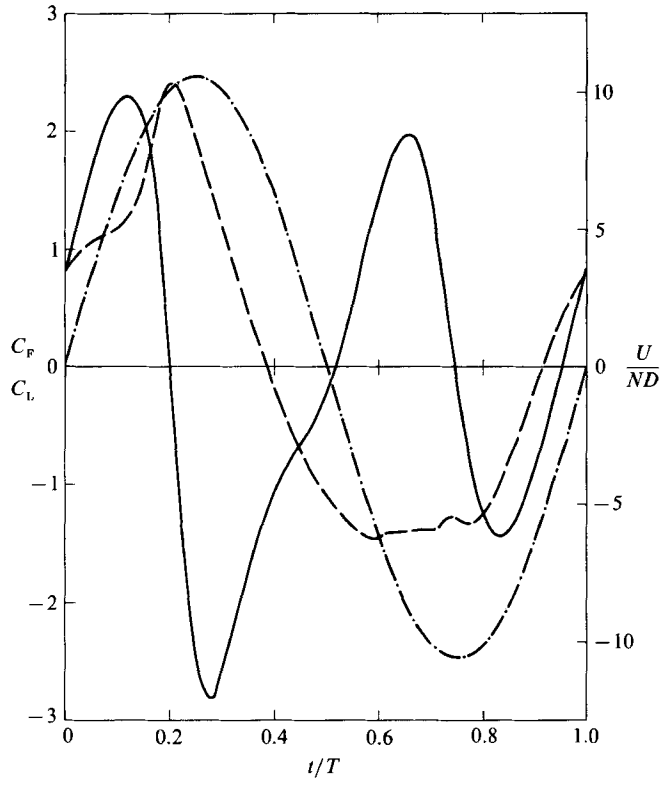

FIGURE 5. Mode-averaged cycles of forces at $KC = 10.6$: — —, in-line force coefficient; ——, transverse force coefficient; — · —, free-stream relative velocity.

simply ensemble-averaged over about 200 cycles and little useful information is obtained since C_L and K_B have averaged to almost zero. The explanation for this is that a mirror-image mode is usually associated with each mode found at $KC = 17.5$. A mode and its mirror-image are shown in figures 6(*b*) and 6(*c*); both generate lift and circulation of roughly the same magnitude but of opposite signs. Figures 9(*a*) and 9(*b*) were recorded at $KC = 15.8$, which is close to the boundary separating the transverse and the diagonal regimes. The figures indicate that the flow switches from one regime to the other. The similarity between the curves of C_L shown in figures 9(*a*) and 5 suggests that $KC = 15.8$ is in the transverse regime whereas comparison of the forms of the C_L curves presented in figures 9(*b*) and 6(*b*) suggests the diagonal regime.

The link between the circulation and the transverse force is exhibited most clearly at $KC = 52.6$ (figure 8) where the dominant frequency of the transverse force is about an order of magnitude higher than the frequency of the bulk flow. The transverse force and the circulation appear to fluctuate in sympathy with each other except during flow reversal when the force drops to zero and changes sign but the circulation remain relatively high. It is interesting to note that the amplitude of the non-dimensional circulation, $K_B = \Gamma_B/U_0 D$, is roughly half that of C_L, and that the lift and the circulation tend to be in phase in the half-cycle where U/ND is negative. Constant circulation during flow reversal is also seen in figures 4, 6(*b*) and 6(*c*). The flow velocity along the sides of the circuit used to measure the circulation does not remain constant during flow reversal. In fact detailed measurements show that there

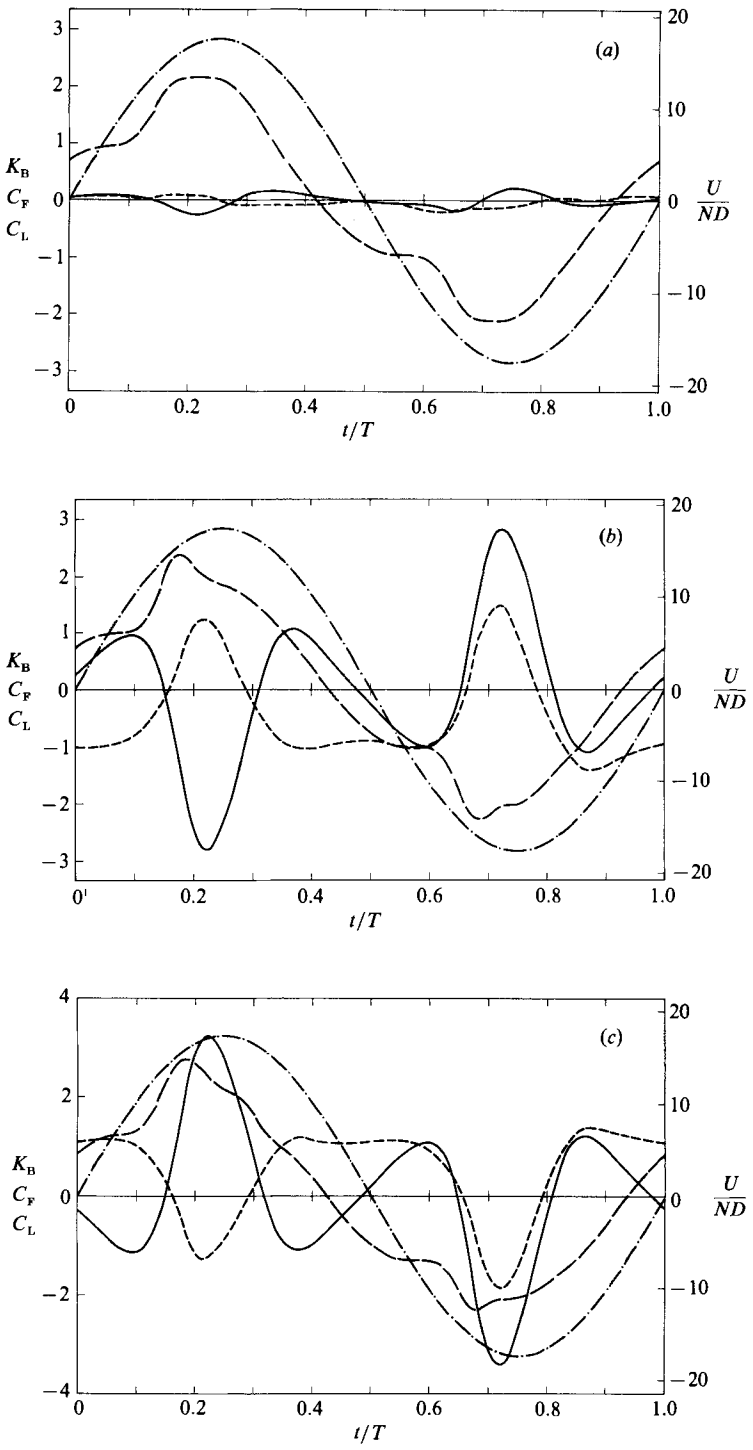

FIGURE 6(*a*). Averaged cycles of forces and circulation at $KC = 17.5$. (*b*) Mode-averaged cycles of forces and circulation at $KC = 17.5$. (*c*) Mode-averaged cycles of forces and circulation at $KC = 17.5$. (Note that this mode is the mirror image of the mode shown in *b*.) — —, in-line force coefficient; ——, transverse force coefficient; – – –, non-dimensional circulation; — · —, free-stream relative velocity.

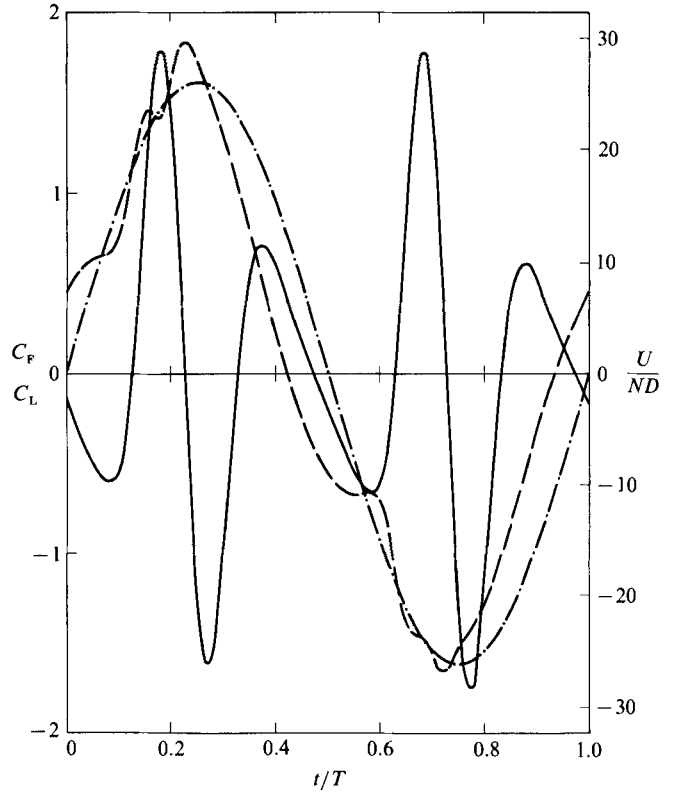

FIGURE 7. Mode-averaged cycles of forces at $KC = 26.2$: — —, in-line force coefficient; ——, transverse force coefficient; — · —, free-stream relative velocity.

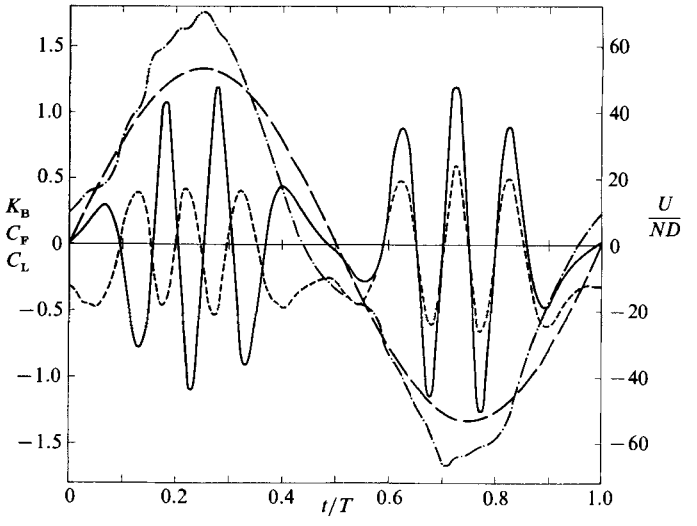

FIGURE 8. Mode-averaged cycles of forces and circulation at $KC = 52.6$. — · —, in-line force coefficient; ——, transverse force coefficient; – – –, non-dimensional circulation; — —, free-stream relative velocity.

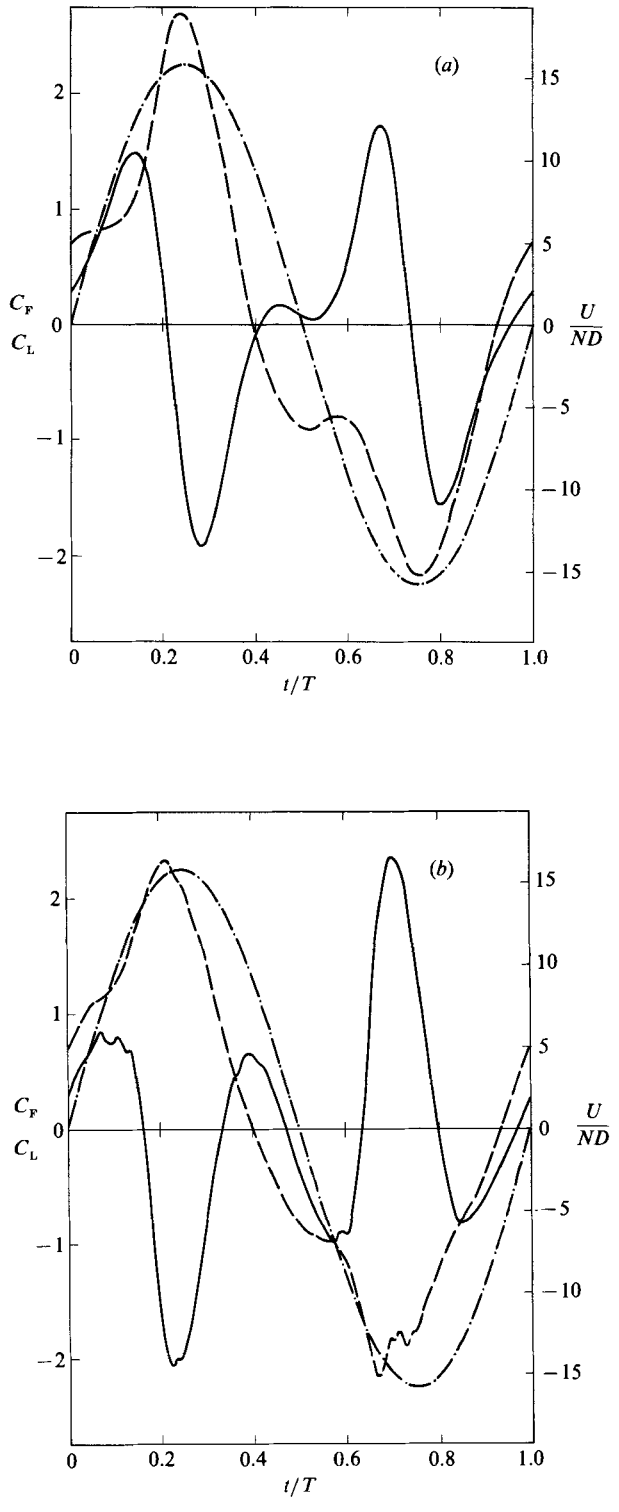

FIGURE 9(*a*, *b*). Mode-averaged cycles of forces at $KC = 15.8$: — —, in-line force coefficient; ——, transverse force coefficient; — · —, free-stream relative velocity.

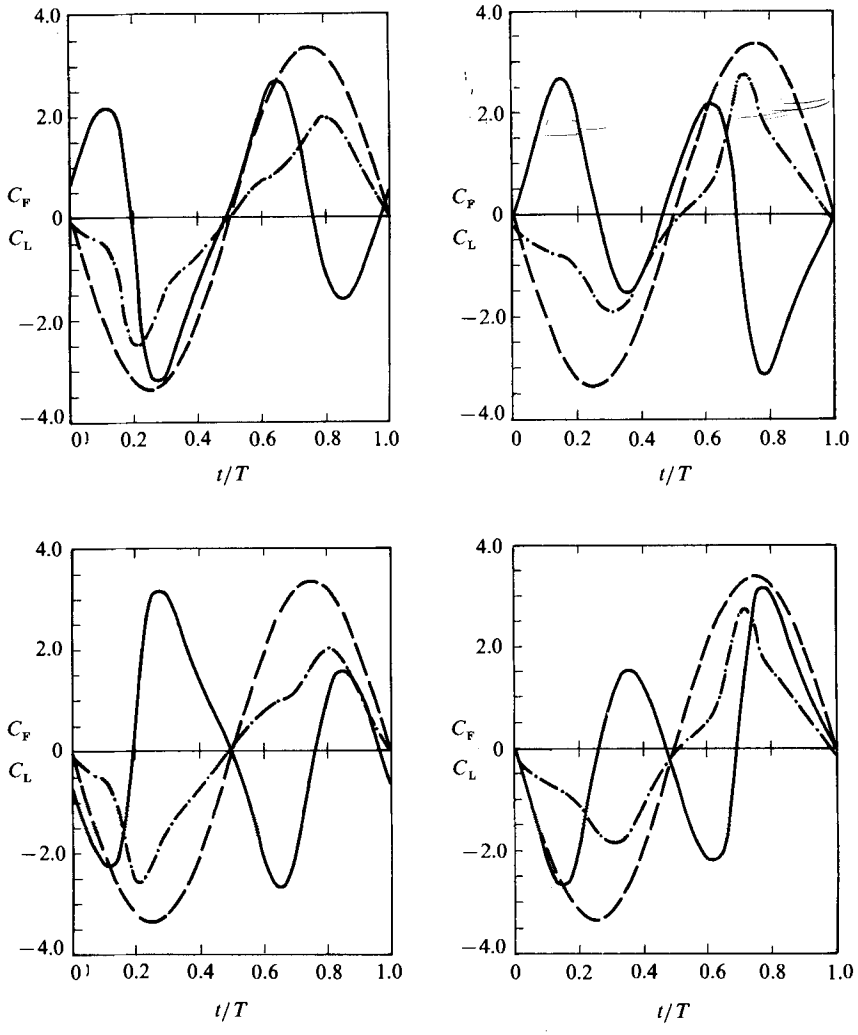

FIGURE 10. Mode-averaged cycles of forces for four vortex modes at $KC = 10$: —·—, in-line force coefficient; ——, transverse force coefficient; — —, free-stream relative velocity.

are very large changes (probably caused by movement of vortices during flow reversal) in the flow along some parts of the circuit, but the circulation around the circuit is conserved.

The measurements associated with the vortex patterns sketched in figures 3(*a*), 3(*b*), and 3(*c*) are presented in figures 4, 5 and 6(*b*) respectively. Using these figures one can relate the generation of forces to the development of vortices. For example when flow reversal occurs as sketched in figure 3 (*c*), that is with the weaker of the two returning vortices being drawn across the back face, figure 6(*b*) indicates that the fluctuating lift changes sign before the main flow reverses. This mode of reversal will be called the normal mode because it seems to occur most often. The mode of reversal in which the stronger vortex is drawn across the back face, as shown in the middle sketch of figure 3(*b*), will be referred to as the cross-mode. Figure 5 indicates that in the cross-mode, the fluctuating lift changes sign after the main flow.

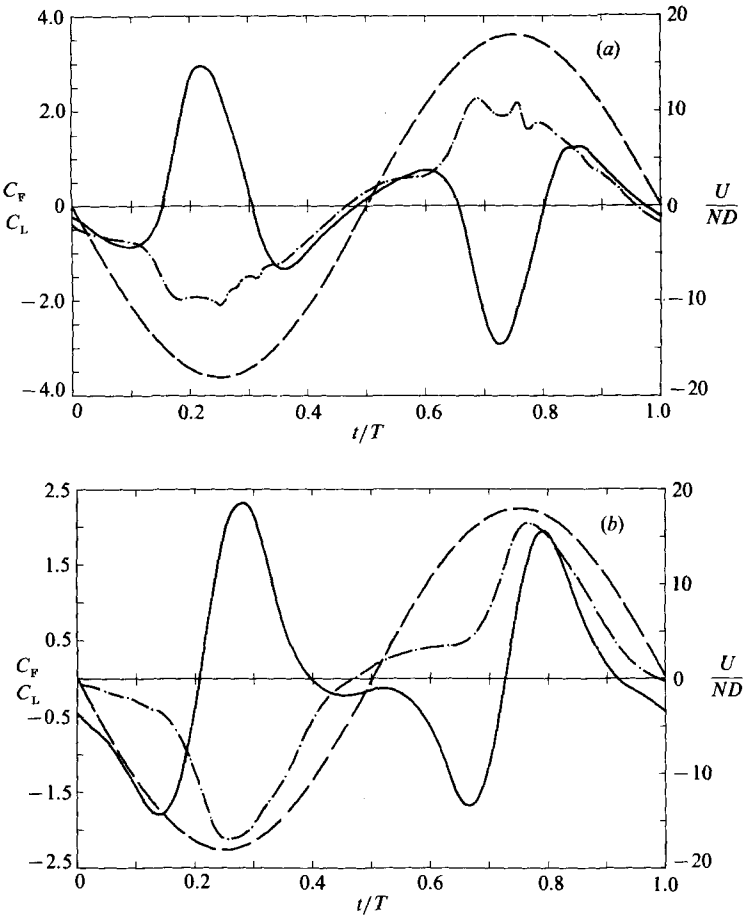

FIGURE 11. Mode-averaged cycles of force at (*a*) low β, (*b*) high β, for $KC = 18$. Notation as in figure 9.

Examples of mode-averaged data recorded in the channel with the cylinder oscillating are shown in figures 10 and 11. That there is close agreement between the transverse forces recorded under similar conditions in the U-tube and the channel can be confirmed by comparing figure 5 and 10 which indicate the same mode. In making this comparison, allowance should be made for the fact that in the first half-cycle of the figures, U is positive in the curve for the U-tube but negative in the curves for the channel. Curves of the in-line forces for the U-tube and the channel are, of course, not directly comparable. Being stationary, the model in the U-tube experiences an additional in-line force (the Froude–Krylov force) associated with the pressure gradient needed to oscillate the fluid.

As reported earlier, four primary modes of vortex shedding can be found in the transverse regime. The curves of C_L and C_F for the four modes are shown in figure 10. It was found that once one of the four modes is established, it is stable. The mode could be changed either by stopping the oscillating model and then starting up the motion again from a stage of rest or by applying a strong perturbation to the flow. Figures 11(*a*) and 11(*b*) indicate that two fundamentally different modes of shedding were found in the channel at $KC = 18$; for $\beta = 634$ (figure 11*a*) the dominant

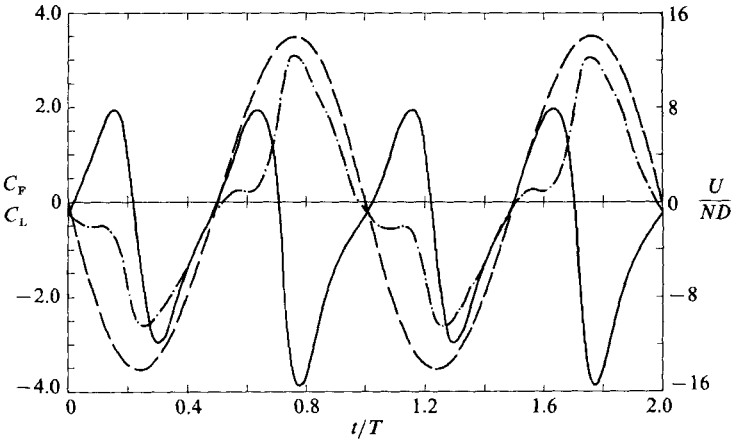

FIGURE 12. Mode-averaged cycles of steady plus fluctuating forces at $KC = 14$. Notation as in figure 10.

frequency of the transverse force is $3N$ whereas for $\beta = 1579$ (figure 11*b*), the dominant frequency is $2N$. This was unexpected because the curve of C_L recorded by Matten, Hogben & Ashley (1979) at $KC \approx 18$ and $R_e = 2.7 \times 10^5$ (i.e. $\beta \approx 15000$) is similar to our curve for $\beta = 634$.

3.3. *Estimation of mean transverse force*

Based on the observation that the vortex activity in the transverse regime takes place mainly on one side of the cylinder, there has been some speculation that the cylinder may experience a steady transverse force in addition to the fluctuating transverse force already shown in figures 5 and 10. To investigate this possibility, the steady part of the pressure-difference signal used to compute the sectional forces was monitored while the side of the cylinder on which the majority of vortex activity was concentrated was switched by perturbing the flow field. These observations were made in the water channel because the flow field could more easily be perturbed in this apparatus. $KC = 14$ was chosen for these experiments because it is close to a boundary of the transverse regime. Vortex patterns are expected to be less stable, and therefore easier to switch, near a boundary. Observations of the pressure difference were again made at twelve angular positions around the cylinder. It was found that when the switch was achieved, the coefficients of the steady component of the sectional transverse and in-line forces changed by 1.08 and 0.06 respectively. (Coefficients are again formed by dividing the sectional force by $\frac{1}{2}\rho U_0^2 D$.) Hence the magnitude of the steady transverse force was estimated to be about 0.5 and that of the steady in-line force to be negligible. Figure 12 shows a mode of the transverse force recorded in the channel at $KC = 14$ with the steady transverse-force coefficient, which for this mode is -0.5, added to the unsteady transverse force.

3.4. *Measurements of forces*

The complete set of in-line force data is shown in figure 13(*a*, *b*) where values of the drag and inertia coefficients calculated from Morison's equation are plotted against KC. The average cycle of the in-line force was formed by ensemble-averaging about 200 successive cycles of the force signal, and C_D and C_M have been calculated from the Fourier coefficients of the part of the force at the oscillation frequency. The

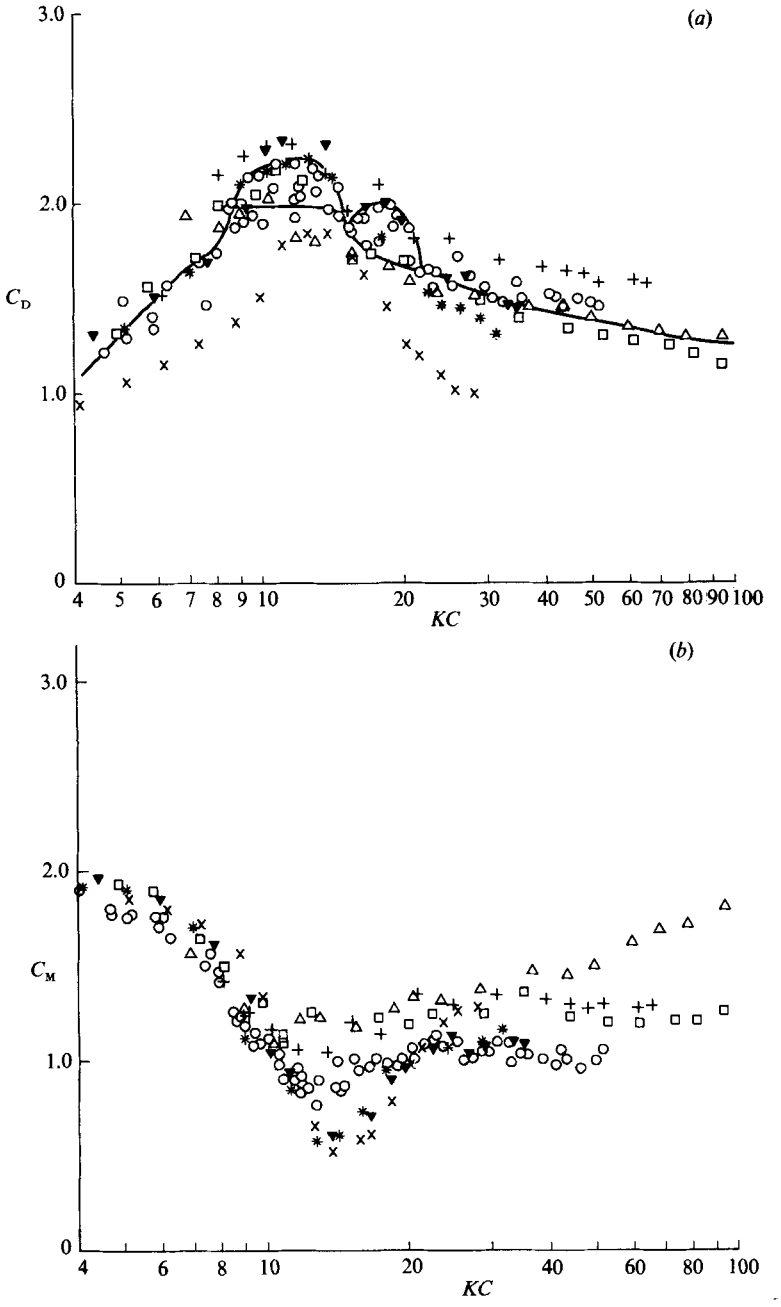

FIGURE 13. (*a*) Drag coefficient versus KC. (*b*) Inertia coefficient versus KC. △, $\beta = 109$; □, 196; +, 301; ○, 483; ▼, 964; *, 1204; ×, 1665.

results shown are for seven values of β, namely 109, 196, 301, 483, 964, 1204 and 1665.

Figure 13(*a*) indicates that there is a range of β in which C_D is not so sensitive to changing β. For $KC \lesssim 30$, the upper boundary of the range lies somewhere between $\beta = 964$ and 1204. It is seen that in the U-tube, C_D can take two values when KC is in the transverse and the diagonal regimes. Some experiments were made in which

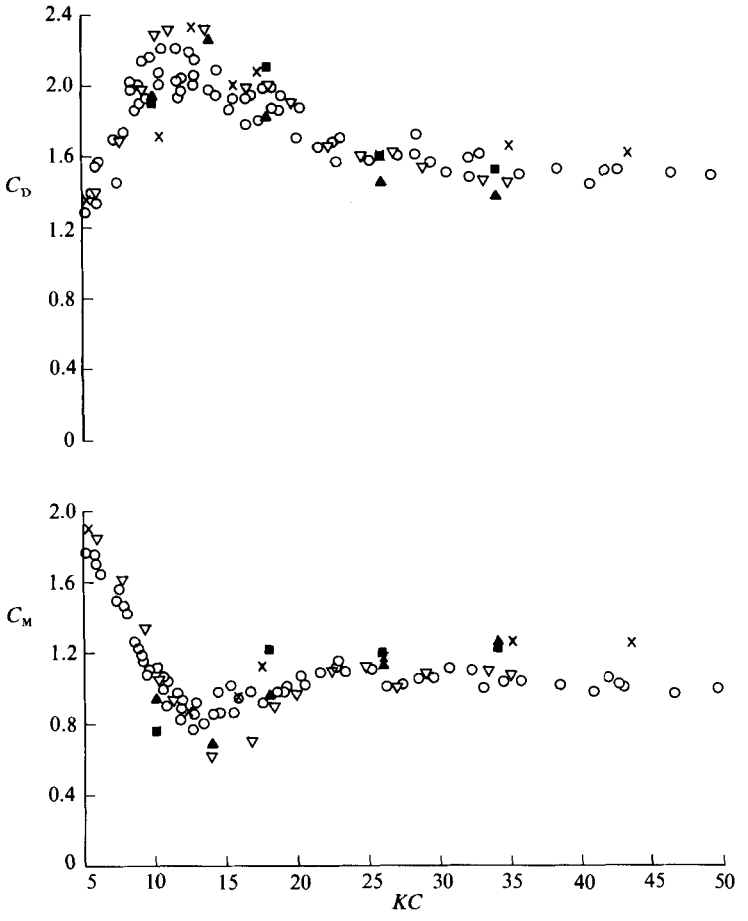

FIGURE 14. Comparison of total force (i.e. strain gauge) and sectional force (i.e. pressure) data. Load cells data: ○, $\beta = 483$; ▽, 964. Pressure data: ×, U-tube, $\beta = 416$; ■, channel, $\beta = 631$; ▲, channel, $\beta = 927$.

the transverse force was monitored at one end of the cylinder while the load cell was in the in-line force direction at the other. These observations suggest that the higher values of C_D occur in runs where the spanwise coherence of vortex shedding is high. For the transverse regime, this suggests that the lower values of C_D are associated with the two-cell structure described earlier.

Values of C_D and C_M calculated from sectional-force (i.e. pressure) measurements in the U-tube and in the water channel are compared in figure 14. The coefficients shown are calculated from the average cycle. The coefficients for the different vortex modes are not shown because they do not differ much from those for the average cycle. In presenting figure 14, one has been added to the C_M values recorded in the channel. Also shown in figure 14 are results obtained in the U-tube from measurements of the total force using the load cells. Generally, the agreement between the different sets of data is very good. At high KC some small differences appear between the channel and U-tube data. In this regard, the influence of the disturbance generated at the free surface of the water in the channel may be important. For although end plates were used, these were of finite size and there will

be a KC value above which the plates can no longer contain the entire flow generated by the oscillating cylinder. That end plates can have a significant influence on the data recorded with a circular cylinder oscillating in still fluid has been demonstrated by Matten *et al.* (1979).

Cycles of the transverse force measured with the load cells were sorted into modes using the basic averaging scheme described in §2.2. For this case, an additional mode-sensor signal is not required; the mode-averaging analysis was performed on the transverse-force signal itself. The coefficient of the transverse force was calculated by dividing the force by $\frac{1}{2}\rho U_0^2 DL$, where L is the length of the cylinder, and the highest magnitude of the coefficient (C_{Lmax}) was determined for each mode. In presenting the results, a mode and the corresponding mirror-image mode are considered as a pair and the higher of the two values of C_{Lmax} calculated for a pair is shown plotted against KC in figure 15(*a*). For this figure, $\beta = 483$ and the symbols used have been chosen so as to indicate the dominant frequencies of the transverse force. For example the figure shows that the dominant frequency is $2N$ at $KC \approx 10$ but can be $6N$, $7N$, $8N$, or $9N$ at $KC \approx 42$, depending on the mode. Also shown in figure 15(*a*) are values of C_{Lmax} obtained from integrated pressure measurements, such as those presented in figures 4–9. In the case of the pressure data, only the predominant mode, and its mirror image, has been considered. Figure 15(*b*) shows the root-mean-square value of the coefficient of the transverse force, C_{Lrms}, for just the predominant mode using the pressure integration technique.

As expected from earlier work (e.g. Sarpkaya 1975; Maull & Milliner 1978; Singh 1979; Ikeda & Yamamoto 1981; Bearman *et al.* 1981; Williamson 1985), there are distinct peaks in C_{Lmax} (figure 15*a*) at values of KC of about 10 and 17. As described by Maull & Milliner (1978) and Williamson (1985), the peak at $KC \approx 10$ is associated with a dominant frequency of $2N$ and that at $KC \approx 17$ with $3N$. At $KC \approx 26$, the location of the third peak in figure 15(*a*), the dominant frequency of the transverse force was found to be $4N$ for about 90% of the cycles examined and $5N$ for only 4% of the cycles. Although a fourth peak at $KC \approx 32$ has been identified by Ikeda & Yamamoto, we found for $KC \gtrsim 32$ that C_{Lmax} decreases more or less monotonically with increasing KC.

Ikeda & Yamamoto (1981) have reported that peaks in C_{Lmax} occur at KC-values where vortex shedding is stable and regular. They suggest that at troughs vortex shedding is unstable and that this is where changes in the vortex regime occur. Based on this criterion, the data in figure 15(*a*) suggests that $KC \approx 14$, 22.8 and 30.5 are possible boundary points between regimes. The boundary separating the regimes can also be inferred from the double-valuedness of C_{D} in both the transverse and the diagonal regimes. This criterion gives (figure 13) $KC = 8.5$, 15 and 22.

3.5. *Correlation of fluctuating transverse force*

Results of correlation measurements made in the channel are presented in figure 16(*a*). They have been calculated, without mode-averaging, from about 200 successive cycles of the data. The correlation coefficient, $R(p, z)$, measured between two sections is plotted against the spanwise separation, z/D, for eight values of KC. $R(p, z)$ is defined as

$$R(p, z) = \overline{P_1' P_2'}/(P_{1\mathrm{rms}} P_{2\mathrm{rms}}),$$

where P_1' and P_2' are the fluctuating parts of the pressure difference recorded at the two sections, $P_{1\mathrm{rms}}$ and $P_{2\mathrm{rms}}$ are the root-mean-square values of P_1' and P_2', and each pressure difference is measured in an axial plane at $\pm 90°$ to the line of motion.

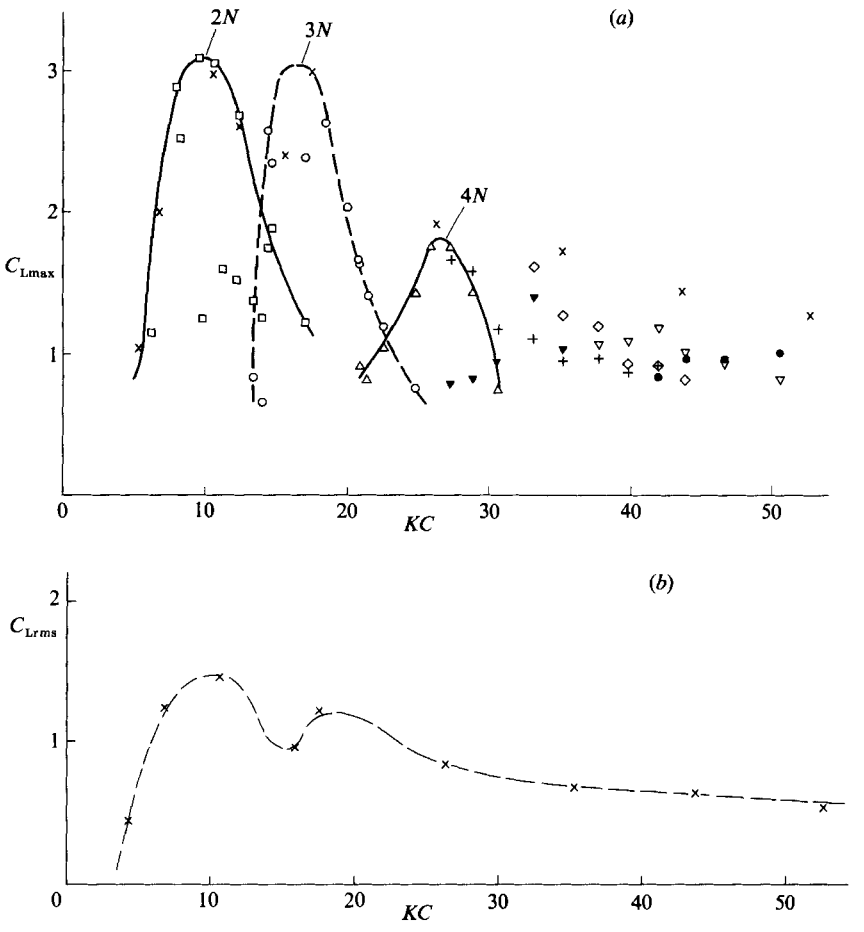

FIGURE 15. (*a*) Mode-averaged C_L versus KC. Symbols and dominant frequency for total force data: □, $2N$; ○, $3N$; △, $4N$; ▼, $5N$; +, $6N$; ▽, $7N$; ●, $9N$. Sectional-force data for the predominant mode: ×. (*b*) Values of C_{Lrms} for the predominant mode, calculated from pressure measurements, versus KC.

Plotted in figure 16(*a*) are curves of $R(p, z)$ recorded at KC-values in the middle of vortex-shedding regimes. Shown for comparison are the results recorded at $KC = 22$, which is near a boundary. In figure 16(*b*) are presented the results recorded at KC-values where boundaries between regimes are expected, together with the results for $KC = 34$. The solid curves in figure 16(*a*, *b*) are given by $e^{-0.215(z/D)}$. Novak & Tanaka (1976) have suggested that a curve of the form $e^{-K(z/D)}$, where K is a constant, can be used to estimate the correlation length of fixed and oscillating circular cylinders in both steady and turbulent approach flows. $R(p, z) = e^{-0.215(z/D)}$ gives a correlation length of $4.65D$ which is similar to the value found on a stationary circular cylinder in steady flow at subcritical Reynolds number.

Results in figure 16(*b*) indicate that the lift is correlated strongly at $KC = 10$ and 18, which are roughly the positions of the first and second peaks in C_{Lmax} (figure 15*a*). For $KC = 10$, $R(p, z)$ is near unity for all values of z/D examined and the two-cell structure found in the U-tube at this KC was not observed in the channel. Figure 16(*a*) shows that the correlation is strong at $KC = 26$, which is roughly the position

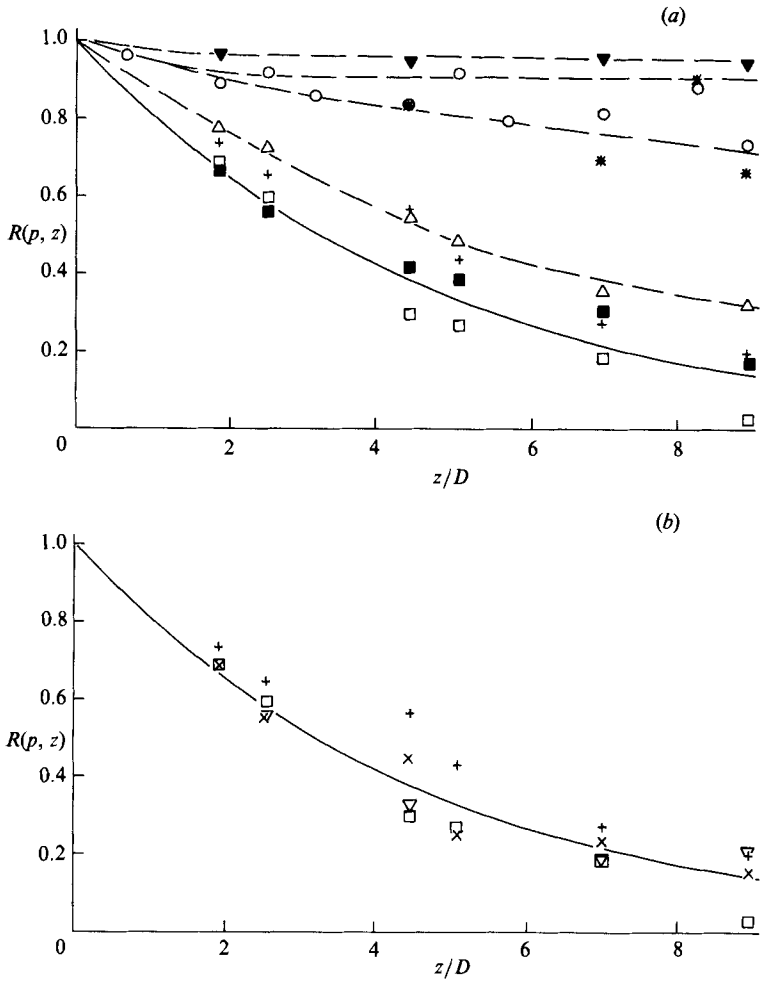

FIGURE 16. Average values of correlation coefficients versus spanwise separation. (*a*) ▼, $KC = 10$; ○, 18; *, 18; □, 22; △, 26; +, 34; ■, 42. (*b*) □, $KC = 22$; ▽, 30; +, 34; ■, 42; ——, $e^{-0.215(z/D)}$. Note $\beta = 683$ except for the case denoted by * where $\beta = 1597$.

of the third peak in the curve of C_{Lmax} versus KC. By contrast the correlation of the lift at $KC = 22$ is particularly poor. That the correlation is lower where there is a trough in the C_{Lmax} curve is also indicated by the fact that the correlation recorded at $KC = 30$ is less than at $KC = 34$ – see figure 16(*b*).

At high KC ($KC \gtrsim 30$), the correlations recorded were similar at all values of KC. It is seen (figure 16*b*) that the empirical curve giving a correlation length of $4.65D$ provides a fairly good fit to the data. This finding adds weight to the argument that the range $KC \gtrsim 30$ can be considered as one vortex-shedding regime (i.e. the quasi-steady).

It was found that at a given KC, a switch in the mode of vortex shedding takes place when the level of the fluctuating pressure difference (and hence transverse force) is low. The change does not occur simultaneously over the cylinder span and for large spanwise separations, instances can be found when the signals are 180° out of phase.

4. Discussion of results

The distinctive features of vortex shedding in planar oscillatory flow have been summarized by Bearman (1985) as follows. Vortex shedding in each half-cycle is initiated by vortices generated in a previous half-cycle and carried back past the body during flow reversal. Vortices convect away from a cylinder by pairing with vortices of opposite sign. Every time KC is increased by about 8 an additional full vortex is shed during a half-cycle and the pattern of shedding is found to change. To this list we add that when KC is high enough for the flow to be asymmetric, vortices of opposite sign are shed alternately. This means that if the last vortex shed in a half-cycle has clockwise circulation, the first vortex shed in the next half-cycle will have anticlockwise circulation.

As reported in the introduction, in the Reynolds-number range studied here a quasi-steady model which assumes a constant Strouhal number $S = 0.2$ can be used to predict the time history of the transverse force on a circular cylinder in planar oscillatory flow. The concept of a constant Strouhal number appears to be confirmed by the finding that an increment of about 8 in KC generates one more full vortex per half-cycle. For suppose that the instantaneous frequency of shedding of vortices of the same sign is SU/D, where U is the instantaneous velocity. Then, using

$$U = \frac{2\pi A}{T} \sin\left(\frac{2\pi t}{T}\right),$$

where A and T are the amplitude and period of the bulk flow respectively, the number, F, of vortices of the same sign shed per cycle is

$$F = \int_0^{2\pi} S \frac{2\pi}{T} \frac{A}{D} \left| \sin\left(\frac{2\pi t}{T}\right) \right| \mathrm{d}t = \frac{2SKC}{\pi}.$$

The number F can be interpreted as the ratio of the mean frequency of vortex shedding during a cycle to the frequency of oscillation of the bulk flow. Since vortices of opposite signs are shed alternately, we deduce from this result that two additional full vortices (one positive and the other negative) are shed per cycle every time KC increases by $\pi/2S$. Using $S = 0.2$, we predict that an additional full vortex is shed per half-cycle when KC increases by 7.85; i.e. roughly 8. At higher Reynolds numbers the value of S used may have to be modified.

An interesting result of the present investigation is that in the transverse vortex regime, the circular cylinder experiences a steady transverse force with a coefficient of about 0.5 at $KC = 14$. The vortex pattern observed in this regime is sketched in figure 3(*b*). One dominant vortex is formed in each half-cycle and the vortex always appears on the same side of the cylinder. This results in the formation of a transverse vortex street on that side of the cylinder (Williamson 1985), and hence there is a mechanism for generating a steady force. It appears that in the U-tube vortex pairs move at about 45° to the direction of the undisturbed stream and are convected by both the main flow and their mutually induced velocity. When the frame of reference is fixed relative to the fluid, it is expected that the path of the vortices will be inclined at more nearly 90° to the line of motion.

Vortex development in the transverse regime is illustrated further by photographs (figure 17, plate 1) taken in the U-tube at $KC \approx 10$ and $\beta = 416$. The flow was visualized by using polystyrene particles. Two narrow slits of light, one orange and the other blue, were projected across the model at roughly a quarter and three-

(*a*)

(*b*)

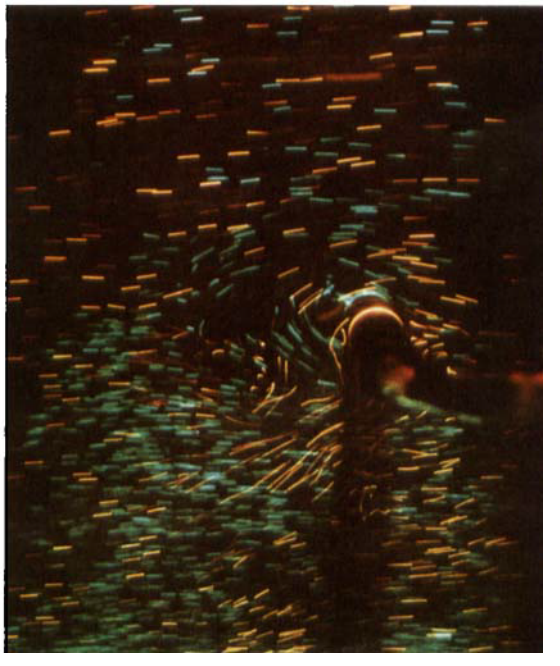

FIGURE 17. Visualization of vortex shedding in the transverse regime at $KC = 10$. Note that different flow patterns are exhibited in the blue and orange view planes.

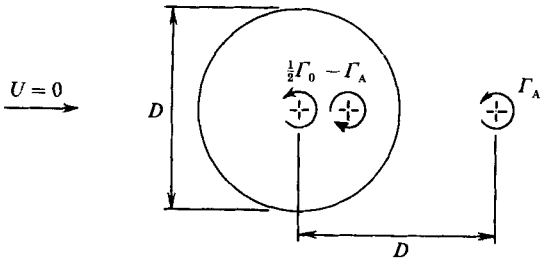

FIGURE 18. Simple model of flow during reversal.

quarter span giving a separation between the view planes of about half the length of the cylinder. In figure 17(*a*) the flow is from right to left and in both view planes, a pair of vortices shed at the bottom of the cylinder is convecting away. The vortices are not very distinct but there is a region of high velocity in between the vortices that is marked by long particle streaks. These streaks give the impression that a jet of fluid has been expelled from the cylinder.

The existence of the two-cell structure described earlier is demonstrated in figure 17(*b*). The flow is again from right to left and in the orange view plane, a pair of vortices shed from the bottom of the cylinder is again convecting away. This time, however, there is no shedding in the blue view plane. That different flow patterns are exhibited in the two planes is evident from the way the long orange streaks left by the shed vortex pair cross the blue streaks. Vortex development in the blue view plane is at the stage indicated by the sketch that is second from the bottom in figure 3(*b*), and shedding will occur at the top of the cylinder when the flow is from right to left. We have no explanation for the formation of this two-cell structure in the U-tube.

The circulation results are thought to merit further consideration if only because such measurements are rarely made. For all the cases examined it was found that at the beginning of a half-cycle the circuit around the cylinder already had a circulation, which in some cases (e.g. figures 4 and 6*b*) could be almost as large as the maximum value obtained during a cycle. At the beginning of a half-cycle vortices are present that have not been convected away by the mechanism of pairing. These vortices and their images in the cylinder influence the future development of the flow.

The role of the image and free circulation in determining the future vortex pattern can be indicated with the aid of a very simple model. It is assumed that the fluid is ideal and that vortices can be represented as point vortices. In steady flow past a cylinder it can be argued that if the strength of a fully formed vortex is Γ_0 then the circulation around the cylinder must fluctuate between $\pm\frac{1}{2}\Gamma_0$, if there is no mean transverse force present. Our measurements of circulation around a circuit surrounding a cylinder indicate that, apart from near flow reversal, vortices of a nearly uniform strength are shed, at values of KC where several vortices are expected per half-cycle (e.g. see figure 8). Near the end of a cycle there may be insufficient time for vortices, still being fed by circulation from the cylinder shear layers, to attain their full strength. Having these factors in mind the simple flow model indicated in figure 18 has been analysed.

The stronger of the two returning vortices is modelled by a point vortex with anticlockwise circulation. Γ_A; for the sake of simplicity, the strength of the weaker vortex is assumed to be negligible compared to Γ_A. Vortices form close to the cylinder

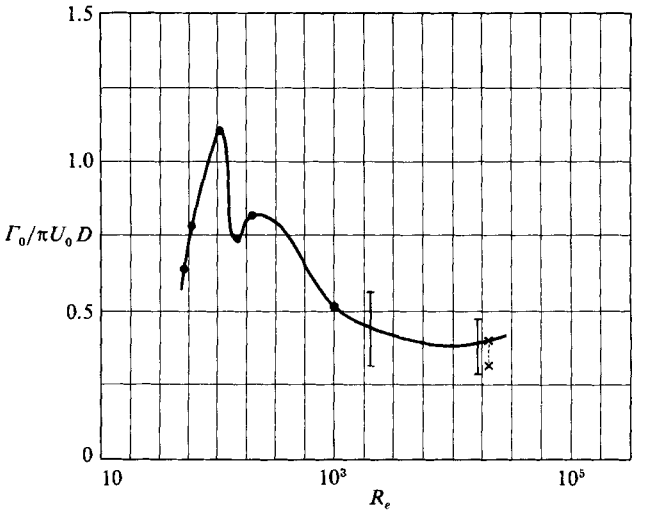

FIGURE 19. Vortex strength versus Reynolds number: ●, I, steady-flow results (Gerrard 1978); ×, oscillatory flow result, $KC = 52.6$.

and have a size of the order of the cylinder diameter, hence it is argued that the (free) vortex can be placed at $x = D$. The image of the free vortex has circulation $-\Gamma_A$ and is positioned at $x = \frac{1}{4}D$. In addition we suggest that there will be a circulation $\frac{1}{2}\Gamma_0$ around the cylinder, where Γ_0 is the strength of a fully formed vortex. Hence the total circulation on the cylinder will be $\frac{1}{2}\Gamma_0 - \Gamma_A$. At flow reversal the vertical component of the velocity of the free vortex in figure 18 is

$$V_A = \frac{\Gamma_0}{2\pi D}(\tfrac{1}{2} - \tfrac{4}{3}\Gamma_A/\Gamma_0).$$

Hence V_A is expected to be positive if $\Gamma_A/\Gamma_0 < 0.375$ and negative if $\Gamma_A/\Gamma_0 > 0.375$.

In figure 18 the flow has been from left to right and since the free vortex has anticlockwise circulation, it must have been formed from the lower shear layer. If V_A is negative we expect the normal mode of reversal with the vortex passing under the cylinder. When it reaches the other side it will have the effect of increasing the velocity near the cylinder and will accelerate the shedding of the next vortex from that side. If V_A is positive we expect the cross-mode with the free vortex passing over the cylinder and enhancing the next vortex to be shed from the top. Although the model presented here can be easily criticised it does suggest that there is a critical vortex strength that determines whether a vortex returns over or under the cylinder. If KC is such that a vortex is close to this critical value then the mode of reversal can be switched either by a small change in the strength or position of the free vortex. We suspect that this is the reason why at some values of KC the shedding mode is stable whereas at others it is unstable.

Returning to the measurements of circulation, it is assumed that the time-mean value of the circulation is zero and that the shedding of vortices of strength Γ_0 leads to a circulation around the cylinder oscillating between $\pm\frac{1}{2}\Gamma_0$. Hence the non-dimensional vortex strength, $\Gamma_0/\pi U_0 D$, is found to range from 0.51 to 0.55, 0.70 to 1.03 and 0.27 to 0.40 for $KC = 6.75$, 17.5 and 52.6 respectively. Since $KC = 52.6$ is

well within the quasi-steady regime, we shall compare the estimate of strength for this KC with steady-flow values. Figure 19 shows that the estimate for $KC = 52.6$ is comparable with, but lies below, the mean of the results for steady flow taken from Gerrard (1978). The oscillatory-flow result seems to be lower because it has been non-dimensionalized by U_0, the maximum value of the free-stream velocity.

In order to compare the vortex strengths estimated at different KC values, vortex strengths were non-dimensionalized by using the maximum velocity of the bulk flow at $KC = 6.75$. The result is that vortex strength still ranges from 0.51 to 0.55 at $KC = 6.75$ but is now 1.81 to 2.67, and 2.10 to 3.12 at $KC = 17.5$ and 52.6 respectively. It is suggested that vortices are tending to grow to more or less the same full circulation and that vortex strength is low at $KC = 6.75$ because, in the asymmetric regime, the full circulation cannot be attained before flow reversal. It is believed that full strength is first attained in the transverse regime. The idea that vortices tend to form to the same strength is supported by the circulation measurements made at $KC = 52.6$. It is seen, particularly in the first half-cycle of figure 8, that over a half-cycle there is not much change in the amplitude of the circulation even though the free-stream velocity varies sinusoidally and vortices are shed from different points in a half-cycle.

We have found that the lift and the circulation around the circuit we have chosen tend to fluctuate in sympathy with each other. This suggests that it might be possible to infer the lift from the circulation and vice versa. To test this possibility, the measured sectional lift is compared in figure 20 with the lift force per unit length, F_L, calculated from

$$F_L = -\rho U \Gamma_B, \tag{4}$$

where F_L, U and Γ_B are instantaneous values of the lift, relative bulk-flow velocity, and circulation respectively. Recall that the sign convention adopted in this paper is that anticlockwise circulation is positive, and positive U is from left to right, i.e. along the x-axis. In steady flow equation (4) is the Joukowski circulation-lift theorem. For $U = U_0 \sin(2\pi t/T)$, the lift coefficient given by (4) is $2(\Gamma_B/U_0 D)$ $\sin(2\pi t/T)$ when the lift force per unit length is non-dimensionalized by dividing by $\frac{1}{2}\rho U_0^2 D$. This and the measured lift coefficient have been plotted against t/T in figure 20 (a–c) for $KC = 6.75$, 17.5 and 52.6. At $KC = 52.6$, there is (figure 20c) a half-cycle where the predicted lift (equation (4)) is in good agreement with measurement. For $KC = 6.75$ and 17.5, the overall agreement is less good but gross features of the curves of the measured lift such as the positions of the peaks and the troughs are still well predicted. It seems that (4) may be considered a good first approximation to the unsteady lift. This is a remarkable finding that we cannot explain and may be fortuitous.

5. Conclusions

The development of flow around a circular cylinder has been investigated in the range of Keulegan–Carpenter number, KC, from about 4 to 55. Following earlier workers, this range is divided into five regimes: $4 \lesssim KC \lesssim 8$, $8 \lesssim KC \lesssim 15$, $15 \lesssim KC \lesssim 22$, $22 \lesssim KC \lesssim 30$ and $KC \gtrsim 30$. These regimes are called the asymmetric, the transverse, the diagonal, the third vortex, and the quasi-steady regimes respectively. In the transverse regime, the cylinder experiences a steady sectional lift force whose coefficient when non-dimensionalized by $\frac{1}{2}\rho U_0^2 D$ is estimated to be 0.5 at $KC = 14$. In this regime, a vortex pair is shed only in one half of a complete flow cycle and the steady lift is associated with the tendency for the shed vortices to form a street on

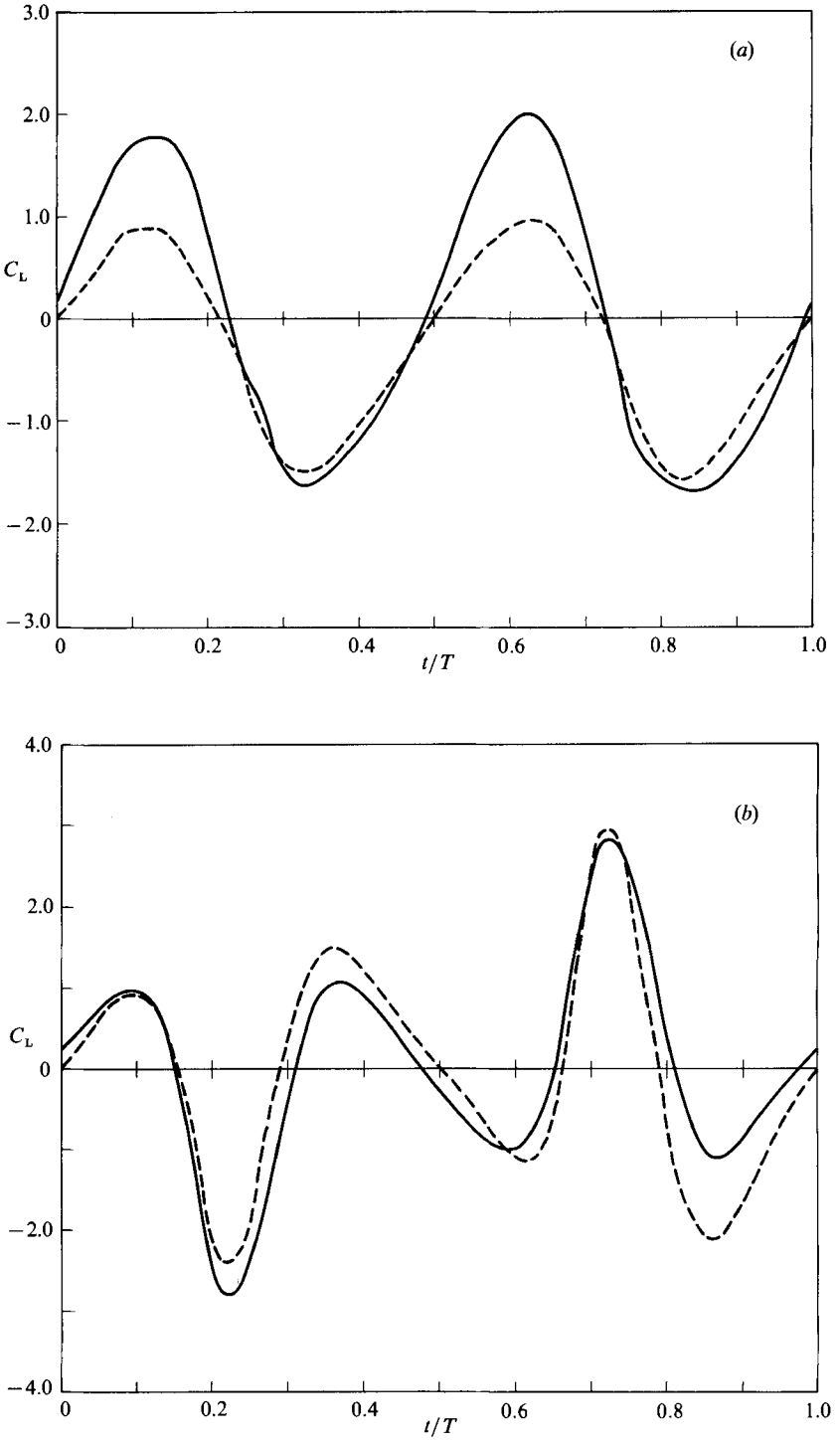

FIGURE 20(a,b). For caption see facing page.

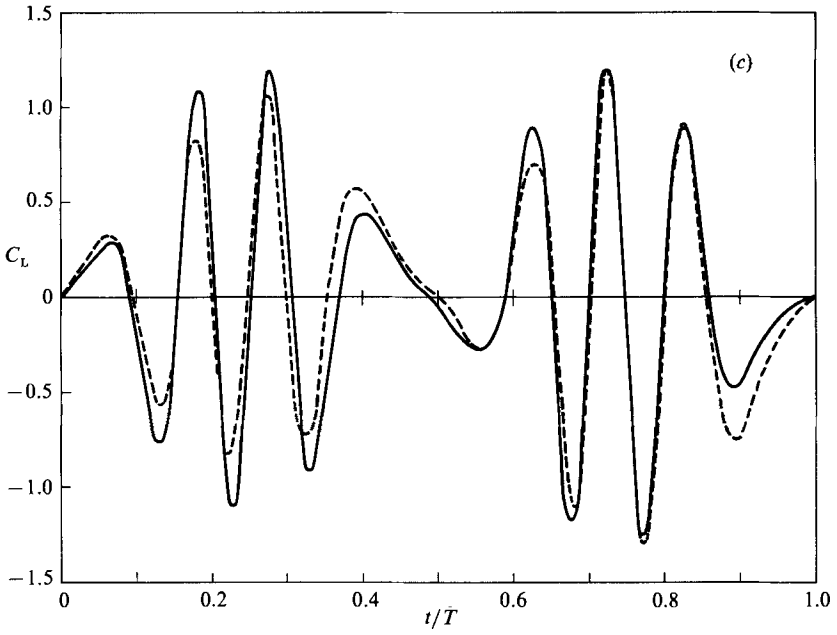

FIGURE 20. Comparison of the measured transverse force with the prediction of the generalized circulation–lift theorem. (*a*) $KC = 6.75$; (*b*) $KC = 17.5$; (*c*) $KC = 52.6$. ——, measured transverse force coefficient; – – –, prediction of the generalized circulation–lift theorem.

one side of the cylinder. Another interesting observation made in the transverse regime is that in the U-tube, vortices were sometimes shed in two cells, each cell occupying roughly half the length of the cylinder.

Cycles of the flow have been sorted according to the mode of vortex formation and for each regime, curves of the time history of the transverse and in-line forces for a typical mode are presented. Corresponding curves of the time history of the circulation around a circuit enclosing the cylinder are presented for the asymmetric, the diagonal, and the quasi-steady regimes. The magnitude of the circulation is found to remain more or less constant during flow reversal. Based on the idea that the shedding of a vortex leads to the generation of a bound vortex of equal strength but of opposite sign, vortex strength $\Gamma_0/\pi U_0 D$ is estimated to range from 0.51 to 0.55, 0.70 to 1.03 and 0.27 to 0.40 at $KC = 6.75$, 17.5 and 52.6 respectively. Using these results we have suggested that in all regimes, fully formed vortices have roughly the same circulation. A remarkable finding is that $\rho U \Gamma_B$ (where Γ_B and U are instantaneous values of an approximation to the circulation around the cylinder and the undisturbed flow relative velocity respectively) is a fairly good approximation to the instantaneous lift.

Measurements show that the spanwise correlation of vortex shedding does not decrease monotonically with increasing KC. For $KC < 30$ the correlation is high at the centre of a vortex regime and low at the ends. For $KC > 30$, the correlation is no longer very sensitive to KC and a curve giving a correlation length of about $4.65D$ provides a fairly good fit to the data.

The work was supported by the Science and Engineering Research Council Marine Technology Directorate. It was completed after one of the authors (E. D. O) had

joined City University. We would like to thank City University for allowing E.D.O. to complete the research.

REFERENCES

BEARMAN, P. W. 1985 Vortex trajectories in oscillatory flow. In *Proc. Intl Symp. on Separated Flow around Marine Structures, Trondheim, Norway, June*, pp. 133–153. Norwegian Hydrodynamic Laboratories, Trondheim, Norway.

BEARMAN, P. W., DOWNIE, M. J., GRAHAM, J. M. R. & OBASAJU, E. D. 1985 Forces on cylinders in viscous oscillatory flow at low Keulegan–Carpenter numbers. *J. Fluid Mech.* **154**, 337–356.

BEARMAN, P. W., GRAHAM, J. M. R., NAYLOR, P. & OBASAJU, E. D. 1981 The role of vortices in oscillatory flow about bluff cylinders. In *Proc. Intl Symp. on Hydrodynamics in Ocean Engng, Trondheim, Norway, August*, pp. 621–635. Norwegian Hydrodynamic Laboratories, Trondheim, Norway.

BEARMAN, P. W., GRAHAM, J. M. R. & OBASAJU, E. D. 1984 A model equation for the transverse forces on cylinders in oscillatory flows. *Appl. Ocean Res.* **6**, 166–172.

GERRARD, J. H. 1978 The wake of cylindrical bluff bodies at low Reynolds number. *Phil. Trans. R. Soc. Lond.* **288**, 351–382.

HONJI, H. 1981 Streaked flow around an oscillating circular cylinder, *J. Fluid Mech.* **107**, 509–520.

IKEDA, S. & YAMAMOTO, Y. 1981 Lift forces on cylinders in oscillatory flows. *Rep. of Dept. Found. Eng. and Const. Eng., Saitama Univ., Japan*, 10, pp. 1–16.

IWAGAKI, Y., ASANO, T. & NAGAI, F. 1983 Hydrodynamic forces on a circular cylinder placed in wave-current co-existing fields. *Memo Fac. Eng., Kyoto Univ. Japan*, vol. 45, pp. 11–23.

KEULEGAN, G. H. & CARPENTER, L. H. 1958 Forces, on cylinders and plates in an oscillating fluid. Natl. Bur. Stand. *J. Res.* **60**, 423–440.

MATTEN, R. B., HOGBEN, N. & ASHLEY, R. M. 1979 A circular cylinder oscillating in still water, in waves and in currents. In *Mechanics of Wave-Induced Forces on Cylinders* (ed. T. L. Shaw), pp. 475–489. Pitman.

MAULL, D. J. & MILLINER, M. C. 1978 Sinusoidal flow past a circular cylinder. *Coastal Engng* **2**, 149–168.

MORISON, J. R., O'BRIEN, M. P., JOHNSON, J. W. & SCHAF, S. A. 1950 The force exerted by surface waves on piles. *Petrol. Trans.* **189**, 149–157.

NOVAK, M. & TANAKA, T. 1976 Pressure correlations on a vibrating cylinder. In *Wind Effects on Buildings and Structures* (ed. K. T. Eaton), pp. 227–232. Cambridge University Press.

SARPKAYA, T. 1975 Forces on cylinders and spheres in a sinusoidally oscillating fluid. *Trans. ASME* E: *J. Appl. Mech.* **42**, 32–37.

SARPKAYA, T. 1976 Vortex shedding and resistance in harmonic flow about smooth and rough circular cylinders at high Reynolds numbers. *Tech. Rep.* NPS-59SL76021. Naval Postgraduate School, Monterey, CA.

SARPKAYA, T. 1986 Force on a circular cylinder in viscous oscillatory flow at low Keulegan–Carpenter numbers. *J. Fluid Mech.* **165**, 61–71.

SARPKAYA, T. & ISAACSON, M. 1981 *Mechanics of Wave Forces on Offshore Structures.* Van Nostrand Rheinhold.

SINGH, S. 1979 Forces on bodies in oscillatory flow. Ph.D. thesis, University of London.

STOKES, G. G. 1851 On the effect of the internal friction of fluids on the motions of pendulums. *Trans. Camb. Phil. Soc.* **9**, 8–106.

VERLEY, R. L. P. 1982 A simple model of vortex-induced forces in waves and oscillating currents. *Appl. Ocean Res.* **4**, 117.

WANG, C.-Y. 1968 On high-frequency oscillating viscous flows. *J. Fluid Mech.* **32**, 55–68.

WILLIAMSON, C. H. K. 1985 Sinusoidal flow relative to circular cylinders. *J. fluid Mech.* **155**, 141–174.